

Discoveries of Diffuse Iron Line Sources from the Sgr B Region

Katsuji KOYAMA, Tatsuya INUI, Yoshiaki HYODO, Hironori MATSUMOTO and Takeshi Go TSURU
Department of Physics, Graduate School of Science, Kyoto University, Sakyo-ku, Kyoto 606-8502
koyama@cr.scphys.kyoto-u.ac.jp, inuit@cr.scphys.kyoto-u.ac.jp

Yoshitomo MAEDA

Institute of Space and Astronautical Science, JAXA, Sagamihara, Kanagawa, 229-8510

Hiroshi MURAKAMI

PLAIN center, ISAS/JAXA, 3-1-1 Yoshinodai, Sagamihara, Kanagawa 229-8510

Shigeo YAMAUCHI

Faculty of Humanities and Social Sciences, Iwate University, 3-18-34 Ueda, Morioka, Iwate 020-8550

Steven E. KISSEL

Kavli Institute for Astrophysics and Space Research, Massachusetts Institute of Technology, Cambridge, MA 02139, USA

Kai-Wing CHAN and Yang SOONG

Code 662, NASA/GSFC, Greenbelt, MD 20771, USA

(Received 2006 July 5; accepted 2006 August 0)

Abstract

The radio complex Sgr B region is observed with the X-Ray Imaging Spectrometers (XIS) on board Suzaku. This region exhibits diffuse iron lines at 6.4, 6.7 and 6.9 keV, which are $K\alpha$ lines of Fe I (neutral iron), Fe XXV (He-like iron) and Fe XXVI (H-like iron), respectively. The high energy resolving power of the XIS provides the separate maps of the K-shell transition lines from Fe I (6.4 keV) and Fe XXV (6.7 keV). Although the 6.7 keV line is smoothly distributed over the Sgr B region, a local excess is found near at $(l, b) = (0^\circ61, 0^\circ01)$, possibly a new SNR. The plasma temperature is $kT \sim 3$ keV and the age is estimated to be around several $\times 10^3$ years. The 6.4 keV image is clumpy with local excesses nearby Sgr B2 and at $(l, b) = (0^\circ74, -0^\circ09)$. Like Sgr B2, this excess may be another candidate of an X-ray reflection nebula (XRN).

Key words: Galaxy:center — ISM:clouds — ISM:individual (Sagittarius B) — X-rays:individual (Sagittarius B) — X-rays:ISM

1. Introduction

Sgr B is a molecular complex consisting of Sgr B1 and B2. In particular, Sgr B2 is the most massive giant molecular cloud with ultra compact H II regions (UCH II) (Gaume et al. 1995) and many maser sources near the cloud center (Mehringer & Menten 1997). These are the hints of high mass (HM) zero age main sequence (ZAMS) stars or young stellar objects (YSOs). However, extremely high absorption toward the cloud center ($N_{\text{H}} \geq 10^{24} \text{ cm}^{-2}$, $A_{\text{V}} =$ a few 100) prevents to detect any stars in optical or even in the infrared bands. Takagi et al. (2002) have discovered many compact X-ray sources in the cloud center with Chandra. The X-ray fluxes and spectra indicate that these are likely HM YSOs. Since HM stars evolve very rapidly and finally undergo supernova explosions, it will be reasonable to expect young SNRs near the Sgr B2 cloud. In fact, Senda et al. (2002) have discovered a peculiar SNR candidate with Chandra.

Sgr B2 is also a strong 6.4 keV line source. Koyama et al. (1996) and Murakami et al. (2001) proposed that Sgr B2 is an X-ray reflection nebula (XRN), irradiated by the Galactic center (GC) source Sgr A*. Sgr A* was then thought to be X-ray bright about 300 years ago, the light traveling time between Sgr B2 and Sgr A*. In this XRN scenario, it is likely that other XRNe will be found in the molecular complex Sgr B. The Suzaku observation on the Sgr B region is intended to discover new SNRs and XRNe. This paper reports the first results of the Suzaku observation.

2. Observation and Data Processing

2.1. Data Collection

The Sgr B region was observed with the XIS on 10-12 October 2005. The XIS consists of four sets of X-ray CCD camera systems (XIS0, 1, 2, and 3) placed on the focal planes of four X-Ray Telescopes (XRT) on board the Suzaku satellite. XIS0, 2 and 3 have front-illuminated (FI) CCDs, while XIS1 has a back-illuminated (BI) CCD. The detail descriptions of the Suzaku satellite, the XRT and the XIS are found in Mitsuda et al. (2006), Serlemittos et al. (2006) and Koyama et al. (2006a), respectively. The XIS observation was made with the normal mode. The effective exposure time after removing the epoch of low earth elevation angle ($\text{ELV} \leq 5^\circ$) and the South Atlantic Anomaly was about 89 ksec.

2.2. The Gain Tuning

In a quick look of the spectrum, we found strong lines at ~ 6.7 keV and ~ 6.4 keV, in everywhere in the CCD imaging area (IA), which may be due to the largely extended Galactic center diffuse X-ray emission (GCDX). These lines are most likely $K\alpha$ lines of Fe XXV (6.7 keV) and Fe I (6.4 keV). Using the center energies of the two strong lines, we made fine correction of the CTI (Charge Transfer Inefficiency), and fine gain tuning in XIS-to-XIS and segment-to-

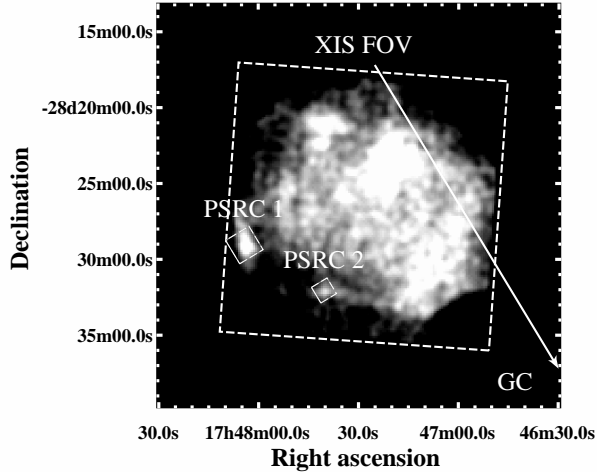


Fig. 1. The X-ray image of the Sgr B region in the 2–10 keV band. All the four XIS data are co-added. The dotted square is the XIS field of view (FOV).

segment levels (relative gain tuning). Then the absolute gain tuning is made using the ^{55}Fe calibration sources irradiating the CCD corners. Details of this procedure and high capability are demonstrated in Koyama et al. (2006b).

2.3. The Position Tuning

After the CTI correction and fine gain tuning, we add all the XIS data and made a composite image of the Sgr B region in the 2–10 keV band (figure 1). The diffuse enhancement in the northwest corresponds to the Sgr B2 complex. Other than this, we found two point sources at the southeast edge of the XIS field of view (FOV). We made the radial profiles of these two sources and determined the peak positions to be $(l, b) = (0^\circ 5762, -0^\circ 1736)$ and $(0^\circ 6626, -0^\circ 2225)$ in the nominal Suzaku coordinate. We search for the Chandra Galactic center survey map, and found possible counterparts, CXO J174741–283213 and CXO J174804.8–282919 (Muno et al. 2003). The Galactic coordinates of these sources are $(l, b) = (0^\circ 5762, -0^\circ 1796)$ and $(0^\circ 6625, -0^\circ 2289)$. Therefore the Suzaku nominal coordinate is systematically shifted by $(\Delta l, \Delta b) = (-0^\circ 0001, -0^\circ 0062)$ from the Chandra coordinate. Since the aspect solution of Chandra is very accurate within sub-arcsec, we made fine tuning of the Suzaku position by shifting $(-0^\circ 0001, -0^\circ 0062)$ in the (l, b) coordinate. Hereafter we use this re-registered coordinate.

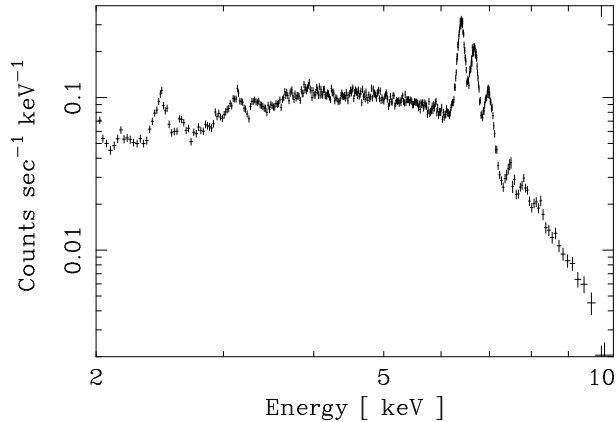


Fig. 2. The X-ray spectra from the full FOV of the XIS, but the CCD corners irradiated by the build-in calibration sources are excluded. All the four XIS data are co-added

3. Results and Discussions

3.1. The Overall Features

The X-ray spectrum of all the Sgr B region is given in figure 2. The spectra of the four XISs (XIS0-XIS3) are co-added and the night earth spectrum (non X-ray background; here, NXBG) is subtracted. With the superior energy resolution of the XIS for diffuse sources, we can clearly resolve the 6.4 keV, 6.7 keV and 6.9 keV lines. These are $K\alpha$ lines from neutral FeI, He-like Fe XXV and hydrogenic Fe XXVI. The 6.9 keV line may contain a small fraction of $K\beta$ line of FeI (7.07 keV). Weak lines seen above 7 keV are $K\alpha$ of NiI (at ~ 7.5 keV), $K\alpha$ of Ni XXVII + $K\beta$ of Fe XXV (at ~ 7.8 – 7.9 keV) and $K\beta$ of Fe XXVI + $K\gamma$ of Fe XXV (at ~ 8.2 – 8.3 keV).

3.2. Discovery of a new SNR

We made a narrow band image of 6.7 keV (the 6.58–6.74 keV band) in figure 3. We see a clear 6.7 keV flux excess at the northwest corner. To confirm the 6.7 keV excess, we referred the archive data of Chandra (OBSID:944, effective exposure time was 99 ksec) and XMM (OBSID: 0203930101, effective exposure time was 42 ksec). Since the energy resolution of the Chandra ACIS is limited to separate the 6.4 and 6.7 keV lines, it is unclear whether the 6.7 keV source is present or not. The XMM image in the 6.7 keV band shows a clear elongated structure near the same position. Accordingly the presence of the 6.7 keV line source is no doubt. On the other hand, the continuum band image (e.g. 2-5 keV, or 2-8 keV bands) shows only a hint of enhancement, and show no clear structure. This source is therefore very peculiar, which is dominant only in the 6.7 keV line. Since the dominance of the 6.7 keV line suggests that the excess is a new SNR (see also below for the discussion), we designate this source as

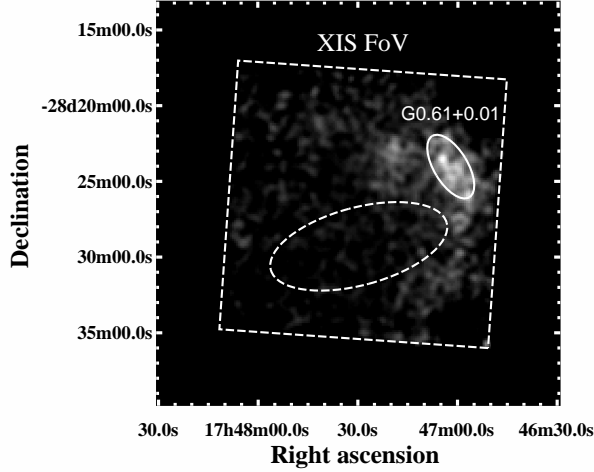


Fig. 3. The 6.7 keV line map (the 6.58–6.74 keV band map) showing bright spot at the northwest corner. The fluxes are normalized by the 6.7 keV flat-field image. The source and background regions are shown by the solid and dotted ellipses, respectively.

Suzaku J1747.0–2824.5 (G0.61+0.01) from its center position.

We made the NXBG-subtracted spectra from the solid ellipse for both the three FI CCDs (XIS0, XIS2 and XIS3 are co-added) and BI CCD (XIS1). In these spectra, the cosmic X-ray background (CXB) and GCDX are still included. We therefore made the NXBG-subtracted spectra from the dotted ellipse in figure 3, and subtract this local background (CXB + GCDX) from the source spectrum. All the spectra have been corrected for the vignetting at 6.7 keV. The results are given in figure 4, for the FIs and BI, separately. We see a pronounced peak at 6.7 keV, but no 6.9 keV line. The 6.7 line shape is asymmetric with a tail at lower energy. In order to verify the line structure, we derive fluxes of the 6.4, 6.7 and 6.9 keV lines ($K\alpha$ line of Fe I, XXV and XXVI) in the source and the background regions, applying a phenomenological model (a bremsstrahlung continuum and many Gaussian lines) in the raw data (no background subtraction). The resulting 6.4, 6.7 and 6.9 keV line fluxes are 2.22, 5.17 and 0.48 for the G0.61+0.01 (source) region, and 0.61, 0.68 and 0.30 for the background region, where the flux unit is 10^{-6} photons cm^{-2} s^{-1} arcmin^{-2} . In contrast to the 6.7 keV line, we see no large excess in the 6.9 keV line from the source region compared to the background region. Thus we confirm that G0.61+0.01 emits strong 6.7 keV line, but very weak 6.9 keV line. The small excess of the 6.4 keV line makes the low energy tail in the 6.7 keV line.

The FI and BI spectra are simultaneously fitted with a plane parallel shock model (VPSHOCK in the XSPEC package) adding two Gaussian lines at 6.4 keV and 7.06 keV. These two lines represent the $K\alpha$ and $K\beta$ lines of Fe I, where the flux of latter line is fixed at 12.5% of the former (Kaastra and Mewe 1993). The best-fit results and parameters are shown in figure 4 and table 1. Although we detected the 6.4 keV line from G0.61+0.01, it is very difficult to judge whether this line is really attributable to G0.61+0.01, due to spilled-over flux from

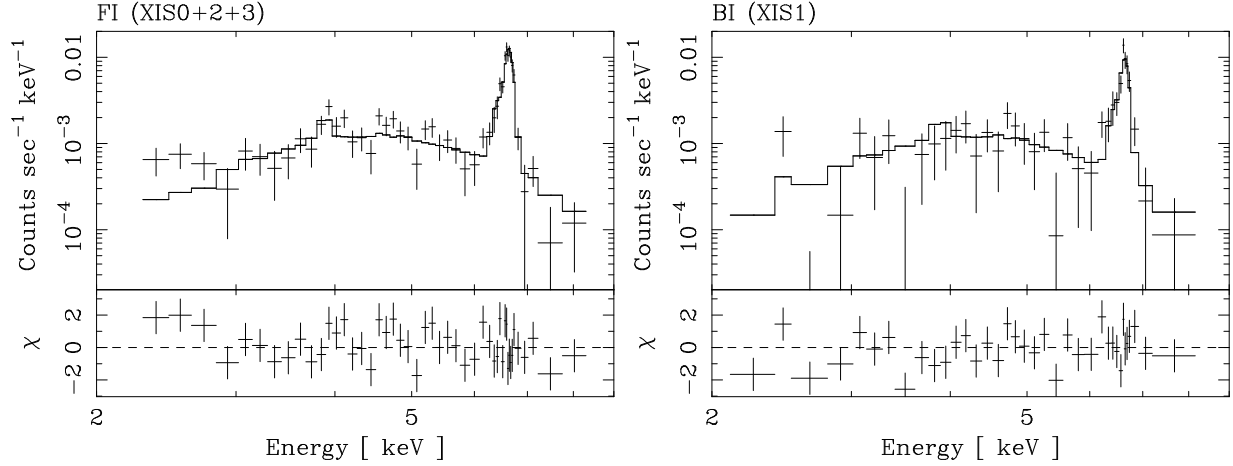


Fig. 4. Left: the X-ray spectrum of the sum of 3 FI CCDs (XIS0, 2 and 3) for a new SNR (G0.61+0.01) with the best-fit VPSHOCK model. Right: same as the left, but of the BI CCD (XIS1)

Table 1. The best-fit parameters for G0.61+0.01 with the VPSHOCK model plus two emission lines

Parameter	Value
N_{H} (10^{23} H cm $^{-2}$)	$1.6^{+0.7}_{-0.4}$
kT (keV)	$3.2^{+2.3}_{-0.9}$
$n_e t$ (10^{11} cm $^{-3}$ s)	$1.9^{+4.7}_{-0.8}$
Abundances*	
Ca	$3.5^{+3.1}_{-2.4}$
Fe	$5.1^{+1.2}_{-1.1}$
Neutral iron lines ^a	
$I_{6.40}$ (10^{-6} photons cm $^{-2}$ s $^{-1}$)	$5.1^{+2.4}_{-2.5}$
$I_{7.06}$ (10^{-6} photons cm $^{-2}$ s $^{-1}$)	0.6
Flux and Luminosity	
F_{2-10}^{\dagger} (10^{-13} ergs cm $^{-2}$ s $^{-1}$)	$7.5^{+1.1}_{-2.2}$
L_{2-10}^{\ddagger} (10^{34} ergs s $^{-1}$)	$1.5^{+0.1}_{-0.2}$
χ^2/dof	99.0/78

Note—The uncertainties indicate the 90% confidence limit.

* The elements which are not listed below are fixed at 1.0 (solar ratio).

^a The line energy of $K\alpha$ and $K\beta$ is fixed at the theoretical value (6.40 and 7.06 keV, respectively; Kaastra and Mewe 1993) and the intensity of $K\beta$ is fixed at 12.5% (Kaastra and Mewe 1993) of that of $K\alpha$.

[†] Observed flux in the 2.0–10.0 keV band.

[‡] Absorption corrected luminosity in the 2.0–10.0 keV band.

the adjacent source Sgr B2, or due to a fluctuation of a larger scale structure in the 6.4 keV line. As for the last possibility, we see a large scale 6.4 keV enhancement in the northwest compared to the background region in the southeast (see figure 5). In any case, we ignore this line in the discussion of G0.61+0.01 because the 6.4 keV line flux is only 3% of that in Sgr B2 (see tables 1 and 3). Since the Suzaku spatial resolution is not good enough, there may be possible contamination of unresolved point sources. To check this problem, we searched for point sources using the Chandra archive data (OBSID: 944, 99 ksec exposure time) and found no point source in the source region. On the other hand, in the background region, there are 48 point sources. The total flux in the 2-10 keV band is 5×10^{-13} ergs cm^{-2} s^{-1} , which is only $\sim 2\%$ of the CXB + GCDX flux of 2.6×10^{-11} ergs cm^{-2} s^{-1} , hence can be ignored in the present data analysis and discussion.

The best-fit temperature of ~ 3 keV and overabundance of Fe are consistent with an ejecta of an SNR and are similar to those found in the central region of Sgr A East, a young SNR near at the GC. The high temperature component of Sgr A East is $kT \sim 4-6$ keV (Sakano et al. 2004, Park et al. 2005, Koyama et al. 2006c), and iron is overabundant by factor of 4-5 (Maeda et al. 2002, Sakano et al. 2004, Park et al. 2005, Koyama et al. 2006c). Thus G0.61+0.01 is likely an ejecta dominant central region of an SNR. We note that Sgr A East has low temperature component of about 1 keV, while not in G0.61+0.01. The absence of softer plasma may be due to the large absorption. The N_{H} value of 1.6×10^{23} H cm^{-2} is larger than that of typical value to the GC (6×10^{22} H cm^{-2}) (Sakano et al. 2002). Therefore, G0.61+0.01 would be located behind or in the rim of the Sgr B2 cloud. Since G0.61+0.01 is located in the south of an expanding radio shell (Oka et al. 1998), which is probably interacting with the Sgr B2 cloud rim, we assume that the distance of G0.61+0.01 is the same as Sgr B2 and to be 8.5 kpc (Reid et al. 1988). Then the 2-10 keV band luminosity is estimated to be 1.5×10^{34} ergs s^{-1} , which is typical for an ejecta plasma of an SNR. The size of G0.61+0.01 (the solid ellipse in figure 3) is $2.2' \times 4.8'$, which corresponds to $5.5 \text{ pc} \times 12 \text{ pc}$ at a distance of 8.5 kpc. Assuming the plasma emission is due to a uniform density ellipsoid with the 3-axis radii of 2.7 pc, 2.7 pc and 6 pc, we estimate physical parameters of G0.61+0.01 (table 2). Although the iron abundance is 3-4 times of the solar, total number and mass of protons are fur larger than those of irons. We therefore assume that electron density (n_e) is equal to the proton density (n_p), and that protons carry most of the plasma mass (m_p). Dividing the radius of the major axis (6 pc) by the sound velocity of the 3.2 keV plasma ($v = 1.4 \times 10^8$ cm s^{-1}), we obtain the dynamical time scale (t_{dyn}) of $\sim 4 \times 10^3$ years. If, instead, we use the ionization parameter ($n_e t$) and electron density (n_e), then the ionization time scale (t_{ioni}) is estimated to be $\sim 7 \times 10^3$ years. Since the source size of $2.2' \times 4.8'$ is comparable to that of the half power diameter ($\sim 2'$), the real size of G0.61+0.01 must be smaller. Therefore the quoted value of $t_{dyn} \sim 4 \times 10^3$ years should be an upper limit, while that of $t_{ioni} \sim 7 \times 10^3$ years is a lower limit, because n_e is inversely proportional to the root square of the plasma volume. Thus the age of G0.61+0.01 is

Table 2. The physical parameters of G0.61+0.01

Parameter	Value
EM ^a (cm ⁻³)	1.4×10^{57}
n_e ^b (cm ⁻³)	0.9
M ^c (M_\odot)	1.3
E ^d (ergs)	2.4×10^{49}
t_{dyn} ^e (s)	1.3×10^{11}
t_{ioni} ^f (s)	2.1×10^{11}

Note—The plasma is assumed to be a uniform density ellipsoid with the 3-axis radii of 2.7 pc, 2.7 pc and 6 pc (see text).

^a Emission measure (EM) = $n_e n_H V = n_e^2 V$, where n_e and n_H are the electron and hydrogen density and are assumed to be equal.

^b The electron density.

^c Total mass (M) = $n_e m_p V$, where m_p is the proton mass and V is the plasma volume.

^d Thermal energy (E) = $3n_e kTV$.

^e The dynamical time scale: the radius of the major axis of the plasma ellipsoid divided by the sound velocity of the ~ 3 keV plasma.

^f The ionization time scale: the ionization parameter (see table 1) divided by the electron density

probably around several $\times 10^3$ years.

Another possibility is that G0.61+0.01 comprises a part of a larger SNR. Since G0.61+0.01 is found at the edge of the XIS field, other parts of a candidate SNR may be out of the XIS field. In this scenario, G0.61+0.01 may be a part of the expanding radio shell discovered by Oka et al. (1998). The kinetic energy of the radio shell is a few of 10^{52} erg s⁻¹, within the range of single or multiple supernova explosions. Thus follow-up X-ray observations including this expanding radio shell is highly required.

3.3. Discovery of a New XRN

We have made a narrow band image at 6.4 keV (the 6.33–6.46 keV band) in figure 5. We see two bright spots in the north. One is Sgr B2 which has been already found as a strong 6.4 keV source (Koyama et al. 1996), and the other is a newly discovered source. We again referred the same archive data of Chandra and XMM as the case of G0.61+0.01. In the Chandra data, this excess is found near the edge of the ACIS FOV. The XMM data show a clear excess near this source. The presence of the 6.4 keV line supports the presence of cool and dense gas clouds. We therefore designate this new source as Suzaku J1747.7–2821.2 (M0.74–0.09) from its peak

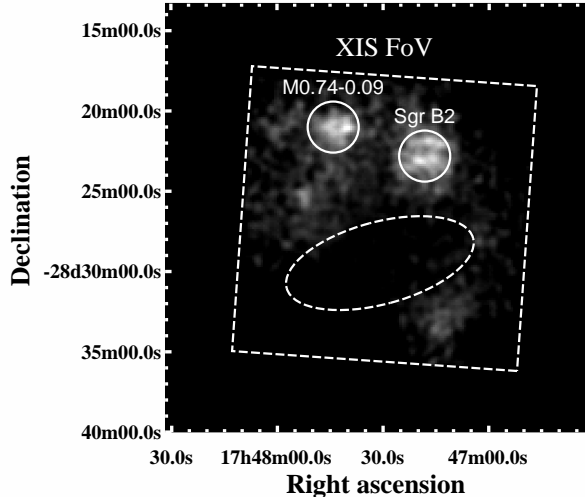


Fig. 5. The 6.4 keV line map (the 6.33–6.46 keV band map) showing bright spots at Sgr B2 and M0.74-0.09. The fluxes are normalized by the 6.4 keV flat-field image. The sources and background regions are shown by the solid circles and dotted ellipse, respectively.

position. We made X-ray spectra of Sgr B2 and M0.74–0.09 from the circles given in figure 5. The former is for comparison to the latter new source. The background spectrum is made from the dotted ellipse and subtracted in the same procedure as the case of G0.61+0.01.

The background-subtracted spectra are shown in figures 6 and 7. We simultaneously fit the FI and BI spectra with a model of absorbed power-law plus two Gaussians near at 6.4 and 7.06 keV, which are for the $K\alpha$ and $K\beta$ lines of FeI. The best-fit parameters are shown in table 3. This model nicely fits the data except an excess near the 6.7 keV line in the Sgr B2 spectra. In fact, the 6.7 keV line map (figure 3) shows a weak enhancement at the position of Sgr B2. One possibility is that the 6.7 keV enhancement is a part of the new SNR candidate G0.61+0.01, because it is located in the close vicinity of Sgr B2. The other possibility is that the 6.7 keV enhancement is due to YSOs embedded in the center of Sgr B2. In fact, the Sgr B2 region is relatively crowded with the Chandra point sources (13 point sources), and at least some of them are YSOs with a hint of the 6.7 keV line emission (Takagi et al. 2002). The total flux (in the 2–10 keV band) of the point sources is $\sim 10^{-13}$ ergs cm^{-2} s^{-1} , which is $\sim 6\%$ of the Sgr B2 flux (see table 3).

The Sgr B2 cloud has been studied extensively with ASCA and Chandra. Koyama et al. (1996) and Murakami et al. (2001) concluded that the 6.4 keV emission is due to fluorescence by strong X-rays coming from Sgr A*, hence named the X-ray reflection nebula (XRN). In this paper, we found a clear $K\beta$ line at 7.06 keV with consistent flux ratio to the $K\alpha$ line (6.4 keV) in the fluorescent X-ray origin and deep Fe edge at 7.1 keV. These discoveries provide additional supports for the XRN scenario of Sgr B2. Further details on the Sgr B2 results with Suzaku will be presented in a separate paper.

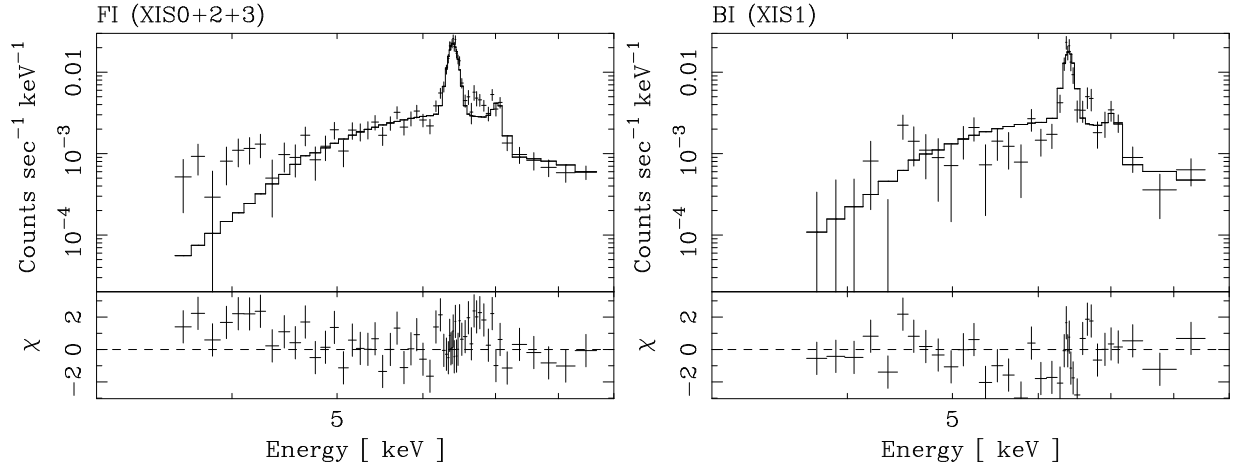


Fig. 6. Left: the X-ray spectrum of the sum of the 3 FI CCDs (XIS0, 2 and 3) for Sgr B2 with an absorbed power-law model and two Gaussian lines. Right: same as the right but of the BI CCD (XIS1)

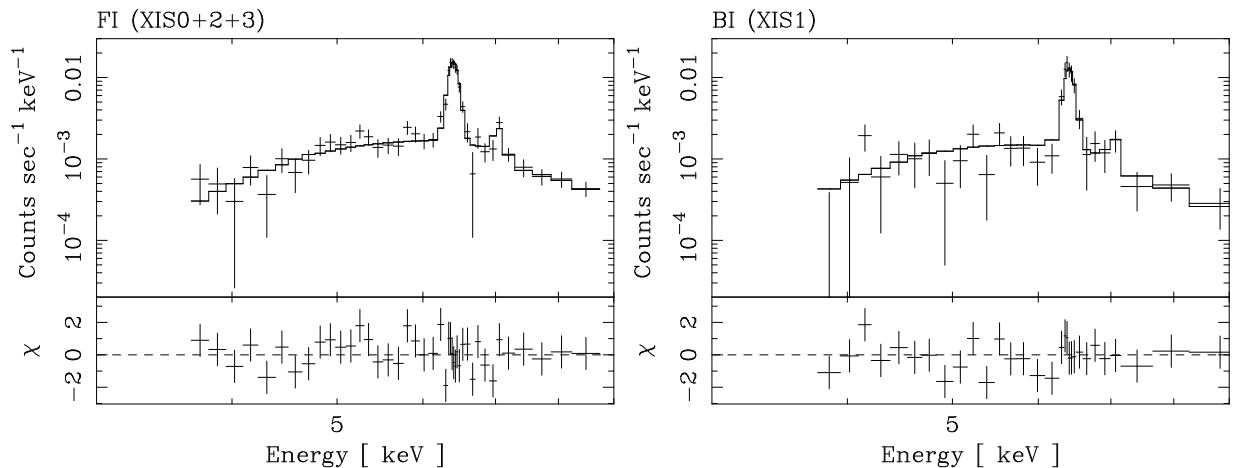


Fig. 7. Same as figure 6, but for a new source M0.74-0.09

In the M0.74–0.09 region, Miyazaki and Tsuboi (2000) reported flux peaks of the CS ($J=1-0$) line emission at $(l, b) = (0^\circ 761, -0^\circ 117)$ and $(0^\circ 764, -0^\circ 064)$, clear evidence for the presence of a molecular cloud. The XIS spectrum of this region exhibits a strong 6.4 keV line with an equivalent width of 1.6 keV, a 7.06 keV line and an Fe edge structure at 7.1 keV (see table 3). All these features are consistent with being from $K\alpha$, $K\beta$ and K-edge from FeI. The flux of the 7.06 keV line is about 10% of that of the 6.4 keV line, which is also consistent with the fluorescent X-ray origin (Kaastra and Mewe 1993). We note here that the background region is the same as the case of G0.61+0.01, hence with the same argument in section 3.2, possible point source contribution can be ignored.

Unlike Sgr B2, no hint of HM YSO is found so far. No bright point source is found in the Chandra image. Therefore, the X-rays can not be the scattering and fluorescence by embedded YSOs. If the X-rays from Sgr B2 and M0.74–0.09 are due to the Thomson scattering and

Table 3. The result of spectral fittings of Sgr B2 and M0.74–0.09 with a power-law and two Gaussian models

Parameter	Sgr B2	M0.74–0.09
Absorbed power-law model:		
Column density N_{H} (10^{23} cm $^{-2}$)	$9.6^{+2.5}_{-0.8}$	$4.0^{+1.4}_{-1.1}$
Photon index Γ	$3.2^{+0.9}_{-0.6}$	$1.4^{+0.4}_{-0.7}$
Gaussian 1 (Fe I K α):		
Line energy (eV)	6399^{+5}_{-5}	6406^{+6}_{-6}
Intensity (10^{-5} photons cm $^{-2}$ s $^{-1}$)	$16.5^{+0.8}_{-0.3}$	$5.9^{+1.4}_{-1.0}$
Equivalent Width (keV)	1.13	1.55
Gaussian 2 (Fe I K β):		
Line energy (eV) ^a	7058	7065
Intensity (10^{-5} photons cm $^{-2}$ s $^{-1}$)	$1.4^{+0.5}_{-0.5}$	$0.6^{+0.3}_{-0.3}$
Equivalent Width (keV)	0.13	0.18
Observed flux [†] (10^{-12} ergs cm $^{-2}$ s $^{-1}$)	$1.5^{+0.1}_{-0.9}$	$1.3^{+0.2}_{-0.8}$
Luminosity [‡] (10^{34} ergs s $^{-1}$)	$9.7^{+0.1}_{-5.1}$	$2.6^{+0.4}_{-0.9}$
χ^2/dof	154.7/89	54.4/66

Note—The uncertainties indicate the 90% confidence limit.

^a The energy gap between K α and K β is fixed at the theoretical value (+659 eV) (Kaastra and Mewe 1993).

[†] Observed flux in the 4.0–10.0 keV band.

[‡] Absorption corrected luminosity in the 4.0–10.0 keV band.

fluorescence of the same irradiating external source like Sgr A*, then the N_{H} ratio between these sources should be similar to the 6.4 keV line flux ratio. The observed N_{H} ratio is 0.42, while that of the 6.4 keV line flux is 0.36, in good agreement of the fluorescence scenario by a single irradiation source. Therefore the XRN scenario by the past activity of Sgr A*, which was successfully applied for Sgr B2 may also be applied for M0.74–0.09.

The counter scenario against the XRN is that the 6.4 keV line emission is produced by the collision of electrons. Since the cross section of iron K-shell ionization is maximum at the electron energy of a few 10 keV (Tatischeff 2002), the most probable source is low energy electrons (LEE) as proposed for the origin of the Galactic Ridge iron K-shell emission (Valinia et al. 2000). Since a few 10 keV electrons are absorbed in less than 10^{22} H cm $^{-2}$ of depth (Tatischeff 2002), the produced X-ray spectrum should have no large absorption edge. Our observation, however, shows a clear absorption of $(4.0\text{--}9.6) \times 10^{23}$ H cm $^{-2}$, in far excess to the Galactic interstellar absorption (Sakano et al. 2002). Thus the LEE origin is unlikely, unless we assume a special geometry such that the 6.4 keV source is deep in or behind the dense cloud.

4. Summary

We summarize the results of the Sgr B observation as follows;

1. All the Sgr B region is covered with a thin hot plasma, which is regarded as a part of the GCDX.
2. The Sgr B region is separately mapped with the 6.4 keV and 6.7 keV lines.
3. We found a local excess in the 6.7 keV line named as G0.61+0.01, which is likely an ejecta dominant SNR.
4. The 6.4 keV map shows local excess at the giant molecular cloud Sgr B2 and M0.74–0.09. Like Sgr B2, M0.74–0.09 is a good candidate of an XRN.

The authors thank all the Suzaku team members, especially T. Takahashi, A. Senda, A. Bamba, J. Kataoka, Y. Tsuboi, H. Uchiyama, H. Nakajima, H. Yamaguchi, and H. Mori for their comments, supports and useful information on the XIS performance. T.I. and H.Y. are supported by JSPS Research Fellowship for Young Scientists. This work is supported by the Grant-in-Aid for the 21st Century COE "Center for Diversity and Universality in Physics" from the Ministry of Education, Culture, Sports, Science and Technology (MEXT) of Japan.

References

- Kaastra, J.S. & Mewe, R. 1993 *A&AS* 97, 443
- Koyama, K., Maeda, Y., Sonobe, T., Takeshima, T., Tanaka, Y., & Yamauchi, S. 1996, *PASJ*, 48, 249
- Koyama, K. et al. 2006a, *PASJ*, in press.
- Koyama, K. et al. 2006b, *PASJ*, in press.
- Koyama, K. et al. 2006b, *PASJ*, in press.
- Gaume, R. A., Claussen, M. J., de Pree, C. G., Goss, W. M., & Mehringer, D. M. 1995, *ApJ*, 449, 663
- Maeda, Y., et al. 2002, *ApJ*, 570, 671
- Mehring, D. M., & Menten, K. M. 1997, *ApJ*, 474, 346
- Mitsuda, K. et al. 2006, *PASJ*, in press,
- Miyazaki, A., & Tsuboi, M. 2000, *ApJ*, 536, 357
- Muno, M. P., et al. 2003, *ApJ*, 589, 225
- Murakami, H., Koyama, K., & Maeda, Y. 2001, *ApJ*, 558, 687
- Oka, T., Hasegawa, T., Sato, F., Tsuboi, M., & Miyazaki, A. 1998, *ApJS*, 118, 455
- Park, S., et al.. 2005, *ApJ*, 631, 964
- Reid, M. J., Schneps, M. H., Moran, J. M., Gwinn, C. R., Genzel, R., Downes, D., & Roennaeng, B. 1988, *ApJ*, 330, 809
- Sakano, M., Koyama, K., Murakami, H., Maeda, Y., & Yamauchi, S. 2002, *ApJS*, 138, 19
- Sakano, M., Warwick, R.S., Decourchelle, A., Predehl, P. 2004, *MNRAS*, 350, 129
- Senda, A., Murakami, H., & Koyama, K. 2002, *ApJ*, 565, 1017
- Serlemittos, P. et al. 2006, *PASJ*, in press,
- Takagi, S., Murakami, H., & Koyama, K. 2002, *ApJ*, 573, 275
- Tatischeff, V. 2002, *astro-ph/0208394*
- Valinia, A., Tatischeff, V., Arnaud, K., Ebisawa, K., & Ramaty, R. 2000, *ApJ*, 543, 733